Applied Catalysis B: Environmental 224 (2018) 500–507

Contents lists available at ScienceDirect

Applied Catalysis B: Environmental

journal homepage: www.elsevier.com/locate/apcatb

Research paper

NiMo-ceria-zirconia catalytic reforming layer for solid oxide fuel cells running on a gasoline surrogate

Kai Zhao[a], Xiaoxue Hou[a], Qusay Bkour[a], M. Grant Norton[a,b,*], Su Ha[a,*]

[a] Voiland School of Chemical Engineering and Bioengineering, Washington State University, Pullman, WA, 99164, USA
[b] School of Mechanical and Materials Engineering, Washington State University, Pullman, WA, 99164, USA

ARTICLE INFO

Keywords:
Internal micro-reformer
Solid oxide fuel cells
Nickel-molybdenum (NiMo) catalyst
Isooctane

ABSTRACT

This paper describes an application of a NiMo-ceria-zirconia (NiMo-CZ) catalyst as a micro-reforming layer for solid oxide fuel cells running on isooctane (i.e., a gasoline surrogate). The catalyst layer was applied on top of a conventional anode supported single cell with a configuration of Ni-yttria-stabilized zirconia (YSZ) anode, YSZ/$Ce_{0.8}Sm_{0.2}O_{1.9}$ bi-layer electrolyte and $La_{0.6}Sr_{0.4}Co_{0.2}Fe_{0.8}O_{3-\delta}$ cathode. Our findings show that the application of the novel catalyst layer was an effective way to reform the mixture of isooctane and air into H_2 and CO, which facilitated the electrochemical oxidation of complex hydrocarbons at the anode. At 750 °C, the single cell with the micro-reforming layer exhibited a low polarization resistance of 1.36 Ω cm^2 and a maximum power density of 405 mW cm^{-2} in the direct feeding condition of an isooctane/air mixture. At the current density of 500 mA cm^{-2}, the cell voltage presented a fairly low degradation rate of 3.0 mV h^{-1} during a 12 h stability test. The excellent electrochemical performance suggests the high catalytic activity of the NiMo-CZ catalyst layer for reforming isooctane and suppressing degradation of the single cell in the direct feeding of isooctane/air.

1. Introduction

Solid oxide fuel cells (SOFCs) are a promising energy conversion device because they can efficiently and directly convert the chemical energy of fuels into electrical energy [1–3]. Due to the high operating temperatures (typically 600–1000 °C), SOFCs hold particular promise because of their ability to use a variety of complex liquid fuels, such as conventional liquid transportation fuels (e.g., gasoline, diesel-like fuels and jet fuels) and next generation liquid bio-fuels (e.g., biodiesel), either by using external reforming systems or directly feeding these fuels to their inexpensive transition metal-based anodes [4,5].

Nickel-based anodes are commonly used in SOFCs due to their low cost, good chemical stability, and excellent catalytic activity toward hydrogen oxidation and reforming of small hydrocarbon molecules. However, the Ni-based anodes are well known for promoting severe surface carbon deposition. Excessive formation of carbon species on the anode leads to a rapid deterioration of the cell performance by physically blocking access of the reactants to the active catalyst sites [6–10].

Recent research indicates that the anode's tolerance to carbon deposition can be improved by substituting the Ni with other metals, such as Cu, Fe and Co [3,11–17]. Among them, Cu-based anodes are found to show high resistance to carbon deposition. Electrochemical performance study indicated that the SOFC single cells employing Cu-Ceria-Yttira-Stabilized Zirconia (YSZ) anode displayed a stable cell voltage at 200 mA cm^{-2} for 12 h in the gasoline operation mode at 700 °C. No evident carbon deposits were observed on the surface of the anode after the performance stability test [16]. In addition, electrochemical performance of the anode has been evaluated using other hydrocarbons (such as methane, *n*-butane and toluene), and stable performances were observed with these hydrocarbons as well [15]. These results demonstrated the high tolerance of the Cu-based anodes to carbon deposition in the presence of complex hydrocarbon fuels.

Despite the excellent performance stability obtained from the Cu-based anodes, the electrocatalytic activity of Cu is quite low, which leads to high electrode polarization resistance and low maximum power density [15,16,18]. In order to maintain good electrochemical activity from the Ni-based anode and high carbon deposition tolerance from the Cu-based anode, Ni-Cu alloys were developed for the anode of direct hydrocarbon SOFCs [13,19,20].

Density-functional theory calculations predicted that alloying Ni with Cu could reduce the carbon and metal binding energy from ~8.7 eV to ~8.1 eV, which could enhance the carbon tolerance of the Ni-based anodes [12]. Experimental research verified the prediction, but the improved carbon tolerance was at the cost of the maximum power density of the cell [13,20]. To utilize the high electrochemical performance of the Ni-based anode and enhance the performance

* Corresponding authors at: Voiland School of Chemical Engineering and Bioengineering, Washington State University, Pullman, WA, 99164, USA.
E-mail addresses: mg_norton@wsu.edu (M.G. Norton), suha@wsu.edu (S. Ha).

http://dx.doi.org/10.1016/j.apcatb.2017.10.067
Received 29 June 2017; Received in revised form 4 October 2017; Accepted 27 October 2017
Available online 31 October 2017
0926-3373/

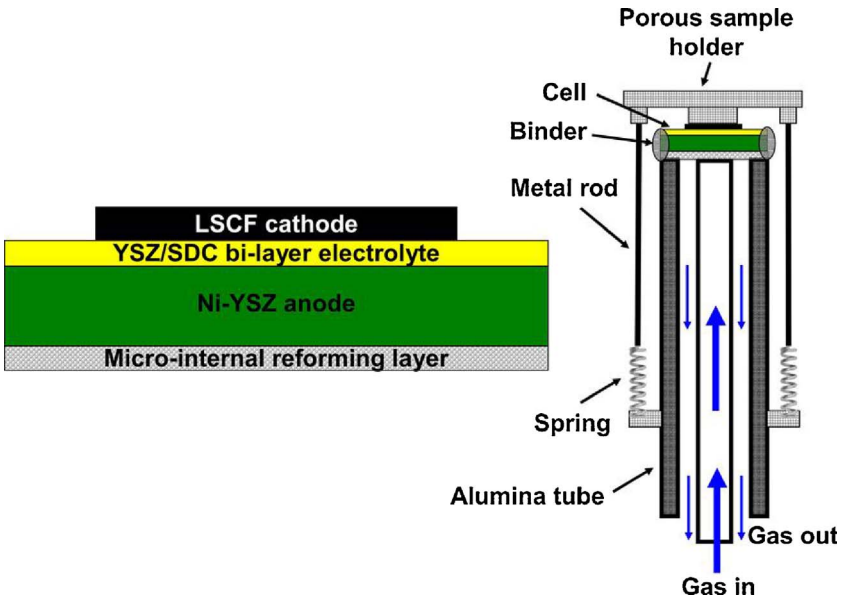

Fig 1. Schematic diagram of the single cell and the experimental setup.

stability in hydrocarbon fuels, an efficient internal reforming single cell design is necessary.

In recent decades, a catalytic reforming layer/anode bilayer design was developed for SOFC single cells running on complex hydrocarbon fuels [21–23]. For this bilayer design, complex hydrocarbon fuels will be reformed to simple syngas (a mixture of hydrogen and carbon monoxide) in the catalytic reforming layer, and the reformed gas will be delivered to the anode for the electrochemical reactions. For the catalytic reforming layer, a high surface area (in an order of 100 $m^2\ g^{-1}$) is essential to efficiently process a large volume of fuel, while the high degree of sintering is indispensable for the anode to efficiently transport electrons and oxygen ions. One single layer cannot maximize both high surface area and a high degree of sintering. On the other hand, the bilayer design can meet these requirements by optimizing one layer for the reforming function and the other layer for the electrochemical function. In order to obtain high reforming efficiency, noble metals (such as Ru and Rh) were used in the internal reforming layer in the previous studies [21,22,24]. For example, a 9.1 wt.% RuO_2-90.9 wt.% Ceria catalyst was applied on Ni-YSZ and Ni-SDC anodes for direct operation in an isooctane and air mixture. By utilizing the catalytic reforming layer, the single cell employing Ni-SDC anode, SDC electrolyte and $La_{0.6}Sr_{0.4}Co_{0.2}Fe_{0.8}O_{3-\delta}$-SDC cathode displayed maximum power density of $\geq$600 mW cm^{-2} at 590 °C and stable performance stability during 50 h operation in isooctane/air [21,22]. In addition, 0.5 wt.% Rh-99.5 wt.% GDC catalyst was applied as a reforming layer in conventional Ni-YSZ anode supported single cells running on *n*-butane at a steam to carbon ratio of 0.5. The cell presented fairly stable performance at 250 mA cm^{-2} during $\geq$200 h operation at 750 °C [23]. The promising electrochemical activity and stability illustrate the feasibility of utilizing the catalytic reforming layer/anode bilayer design for the SOFCs. Despite the excellent electrochemical performance obtained using the catalytic reforming layer, the use of noble metals (either Ru or Rh) would significantly increase the overall cost. Thus, an alternative and inexpensive catalytic material with high reforming activity and good stability is required to operate the Ni-based anode in complex hydrocarbon fuels.

In previous work, our group successfully synthesized a NiMo-ceria-zirconia catalyst that displayed not only high reforming activity for various liquid hydrocarbons, but also excellent coking tolerance [25]. In the present paper, we applied the NiMo-ceria-zirconia catalyst as an internal micro-reformer for conventional Ni-YSZ anode supported single cells. Effects of the micro-reforming layer on electrochemical performance of the single cells were comparatively investigated by running the cell with an isooctane/air mixture as fuel. After the electrochemical performance measurement, the anodes were characterized using various analytical techniques including X-ray diffraction (XRD), and scanning electron microscopy (SEM) with energy dispersive X-ray analysis (EDX).

2. Experimental

2.1. Synthesis of catalyst

Commercial ceria-zirconia ($CeO_2{\cdot}ZrO_2$ (CZ), Sigma-Aldrich) was used to prepare NiMo-CZ (Ni: 11 wt.%, Mo: 3 wt.% and CZ: 86 wt.%) by the wet co-impregnation method. An aqueous solution ($Ni(NO_3)_2{\cdot}6H_2O$: 0.85 mol L^{-1} and $(NH_4)_6Mo_7O_{24}{\cdot}4H_2O$: 0.021 mol L^{-1}) was mixed with the CZ powder at 70 °C. The mixture was then dried at 100 °C for 12 h followed by calcining at 500 °C for 4 h in air. Finally, the powder was reduced at 750 °C for 1.5 h in 50% hydrogen diluted with helium. The resulting powder is referred as NiMo-CZ.

2.2. Single cell fabrication

Anode supported coin-type single cells with a configuration of porous NiO-YSZ anode supporter/YSZ/$Ce_{0.8}Sm_{0.2}O_{1.9}$ (SDC) bi-layer electrolyte/$La_{0.6}Sr_{0.4}Co_{0.2}Fe_{0.8}O_{3-\delta}$ (LSCF) cathode were fabricated by a dry-pressing and spin-coating process. The detailed fabrication procedure was reported in our previous paper [26].

The micro internal reforming layer was deposited onto the porous YSZ substrate by painting. The 75 wt.% YSZ power was mixed with 25 wt.% corn-starch by ball milling in ethanol. After drying, the mixed powder was pelletized into ceramic discs and sintered at 1400 °C for 4 h in air. The porosity of the YSZ substrate was determined to be ~30% by the Archimedes' method. The catalyst paste was prepared by mixing 20 wt.% NiMo-CZ powder with a slurry containing 2.4 wt.% binder (Butvar B-98, Sigma-Aldrich) and 77.6 wt.% ethanol (Decon Labs Inc). A total amount of 20 mg NiMo-CZ catalyst was painted on both surfaces of the porous YSZ substrate to form the micro internal reforming layer. As illustrated in Fig. 1, this internal reforming layer was physically attached to the anode of the single cell using compression springs and ceramic binder for electrochemical performance evaluation.

2.3. Structural characterization

The microstructure of the Ni-YSZ anode supported single cell and

the catalytic internal reforming layer were examined by SEM, (FEI Sirion). Carbon species deposited on the Ni-YSZ anode was investigated by SEM/EDX analysis after electrochemical performance measurements.

2.4. Cell performance investigation

Electrochemical performance of the anode supported single cells with the NiMo-CZ catalytic reforming layer were characterized using a lab-designed fuel cell testing system. The system consisted of an Autolab electrochemical workstation (Metrohm Autolab M101), a DC electric load (BK precision 8500), and a set of mass flow controllers (Brooks 8580E) and alumina sample holders. An alumina-based ceramic binder (AREMCO Products) was used as the gas sealing material. The single cell was heated to 800 °C and the anode was reduced in hydrogen. The open circuit voltage (OCV) of the cell was recorded as a function of time. After the OCV of the cell reached a steady state, the temperature of the cell was cooled to 750 °C for electrochemical performance measurements. The performance of the single cell was first tested using hydrogen (50 sccm hydrogen and 50 sccm nitrogen) as fuel. Then, the fuel was changed to a mixture of isooctane and air by flowing air through an isooctane bubbling system at a flow rate of 100 sccm at 25 °C. The molar ratio of isooctane to air was measured to be 1:20, which is comparable with previously published data with a similar experimental setup [22]. Electrochemical impedance spectra of the single cell were obtained under the OCV condition in the frequency range of 0.01 Hz to 100 kHz. The amplitude of the input sinusoidal signal was set to be 10 mV.

Reforming properties of the catalyst layer were evaluated under OCV condition using the single cell setup as illustrated in Fig. 1. The inlet flow rates of gases were adjusted by the mass flow controllers and compositions of the tail gas were analyzed by gas chromatography (SRI 8610C). The carbon conversion, H_2, CO and CH_4 yields were calculated by the following equations:

$$\text{C conversion} = (\text{total mole number of CO, } CO_2 \text{ and } CH_4)/(8 \times \text{mol number of isooctane fed in}) \quad (1)$$

$$H_2 \text{ yield} = (2 \times \text{mol number of } H_2)/(18 \times \text{mol number of isooctane fed in}) \quad (2)$$

$$\text{CO yield} = (1 \times \text{mol number of CO})/(8 \times \text{mol number of isooctane fed in}) \quad (3)$$

$$CH_4 \text{ yield} = (1 \times \text{mol number of } CH_4)/(8 \times \text{mol number of isooctane fed in}) \quad (4)$$

Performance stability of the single cell was evaluated at 750 °C in the mixture of isooctane/air. The performance stability was tested by monitoring voltages of the single cell at a constant current density of 500 mA cm^2.

3. Results and discussion

3.1. Structure investigation

Fig. 2 shows a XRD pattern of NiMo-CZ powder in the 2θ range from 20 − 80°. Characteristic diffraction peaks for the cubic NiMo solid solution and CZ phases were identified. The main peak for the NiMo solid solution phase (2θ = 43.91°) was shifted towards the lower 2θ region compared with the single Ni phase (2θ = 44.505°, JCPDS No: 04-0850). This shift is due to the incorporation of the larger Mo atoms (1.45 Å) into the cubic Ni (1.35 Å) phase, leading to the expansion of the Ni lattice parameter [27]. This NiMo-CZ powder was used to prepare the micro internal reforming layer for Ni-YSZ anode supported single cell.

Fig. 3 shows SEM images of the single cell at different magnifications and the corresponding EDX mapping image. Thicknesses of the YSZ layer, SDC layer and the LSCF layer were determined to be

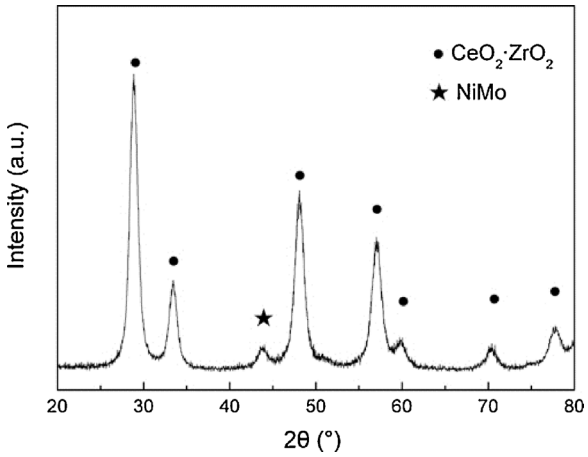

Fig. 2. XRD pattern of NiMo-CZ catalyst at 2θ range of 20–80°.

11 ± 3, 4 ± 1, and 19 ± 2 μm, respectively. EDX mapping indicated no significant inter-diffusion at the interfaces.

3.2. Reforming property

For the NiMo-CZ catalytic reforming layer/Ni-YSZ anode bilayer single cell, the catalytic reforming layer is designed to reform the mixture of isooctane and air into syngas. To validate the hypothesis, we measured the composition of the tail gas from anode channel under OCV condition. Fig. 4 shows reforming properties of the cell in isooctane/air at 750 °C. Without the catalyst layer, the carbon conversion was only 52%, and the hydrogen and carbon monoxide yields were 14% and 10%, respectively. With the application of the catalyst layer, the carbon conversion increased to 71%. Although not all the fuel was converted to syngas, the hydrogen yield increased by 2.3 times and the carbon monoxide yield displayed an increment of 3.4 times. The improved syngas yield demonstrated the effectiveness of the catalyst layer for reforming the isooctane/air mixture.

3.3. Electrochemical performance

Fig. 5(a) shows voltage and power density of the Ni-YSZ anode supported single cell as a function of the current density at 750–800 °C in hydrogen fuel. An OCV value of 1.00 V was obtained at 800 °C, indicating good sealing by the ceramic sealant. When decreasing the operation temperature from 800 to 750 °C, the OCV slightly increased to 1.02 V. The variation of OCV was in agreement with previous experimental data on a SOFC single cell using a Ni-based anode and theoretically predicted data [28]. At 800 °C the single cell exhibited a maximum power density (MPD) of 670 mW cm^{-2}, comparable with previous research results on Ni-based anode supported single cells [28].

Fig. 5 (b) shows Nyquist plots of the single cell under the OCV condition in hydrogen fuel. The impedance spectra were fitted by the equivalent circuit model ($LR_{ohm}(R_HQ_H)(R_LQ_L)$, shown in the inset of Fig. 5 (b)) using Zview software. The inductance element L represents the inductive impedance response, while R_{ohm} is the ohmic resistance of the entire cell. $(R_HQ_H)(R_LQ_L)$ components denote the electrochemical processes from both the anode and the cathode. R is the resistance and Q is the constant phase element. The subscript H and L denote the electrochemical processes from high frequency arc and low frequency arc, respectively. The impedance Z_Q of a constant phase element Q and the equivalent capacitance C of different electrode processes can be calculated according to the following equations:

$$Z_Q = 1/[Q(i\cdot 2\pi f)^n] \quad (5)$$

$$C = (R\cdot Q)^{1/n}/R \quad (6)$$

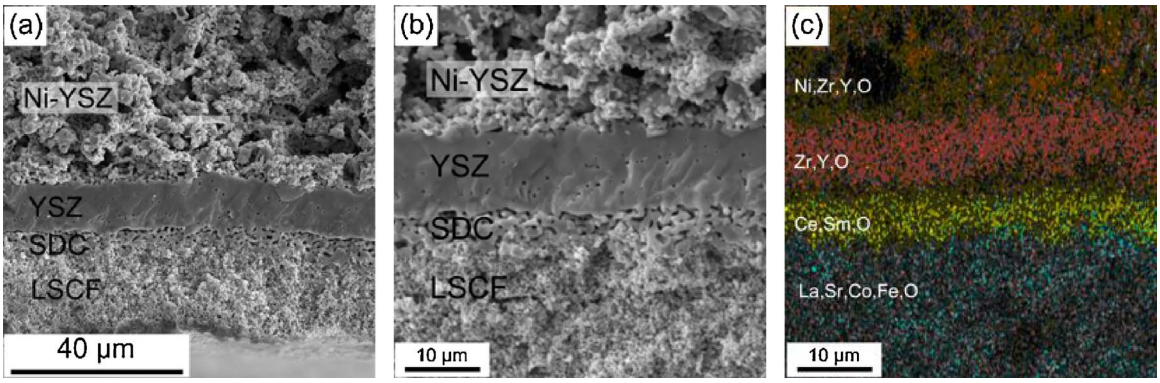

Fig. 3. SEM images of the single cell: (a) low magnification image, (b) higher magnification image, and (c) EDX mapping from (b).

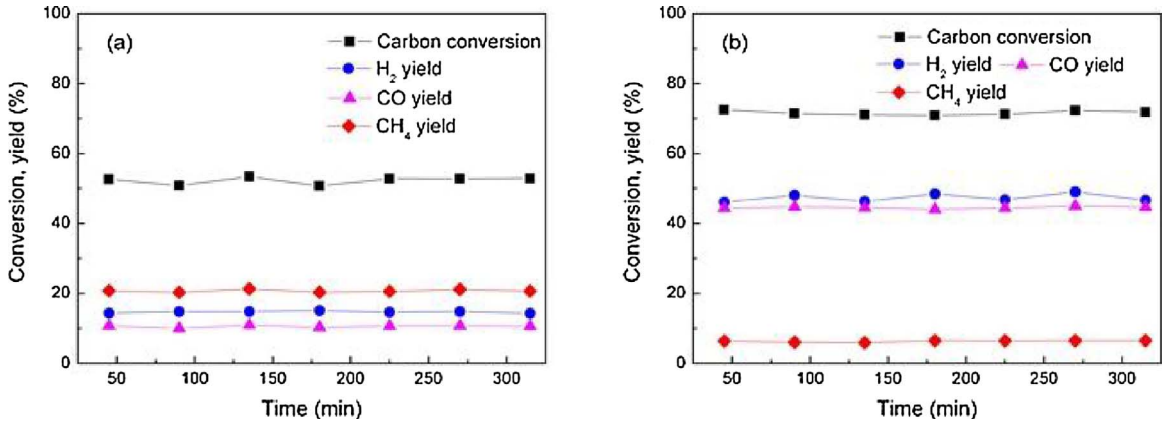

Fig. 4. Tail gas compositions from anode channel of the single cell: (a) without the catalyst layer and (b) with the catalyst layer at 750 °C.

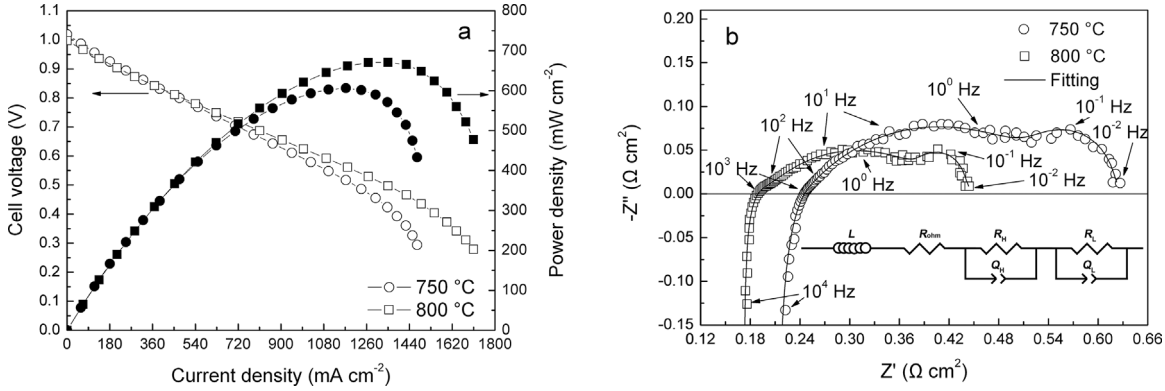

Fig. 5. (a) Voltage and power density of the single cell without the micro-reforming layer at different current densities in hydrogen, and (b) Nyquist plots of the single cell under the OCV condition. The equivalent circuit model is shown in the insert of (b).

Table 1
Electrochemical parameters of the single cell without the micro-reforming layer.

Temperature (°C)	Fuel	R_{ohm} (Ω cm^2)	R_H (Ω cm^2)	R_L (Ω cm^2)	R_p (Ω cm^2)	MPD (mW cm^{-2})
800	Hydrogen	0.17	0.24	0.04	0.28	670
750	Hydrogen	0.21	0.35	0.07	0.42	606
750	Isooctane/air	0.22	0.32	1.45	1.77	392

The equivalent capacitance associated with the high frequency arcs were on the order of magnitude of 10^{-2} F cm^{-2}. Thus, the polarization resistance corresponding to the high frequency arc (R_H) can be ascribed to the electron charge transfer process on the surface of the electrodes [29–31]. The equivalent capacitance for the low frequency arcs were on the order of magnitude of 10^0–10^2 F cm^{-2}. According to previous research on mechanisms of electrochemical reactions on SOFCs, such large equivalent capacitance could be due to gas adsorption and dissociation, and gas diffusion processes in the porous electrodes [29,32,33]. Hence, R_L can be regarded as the polarization resistance from these processes. The polarization resistance of the entire cell (R_p) is the sum of R_H and R_L.

The electrochemical parameters obtained from impedance spectra fittings are listed in Table 1. With the reduction of the operation temperature from 800 to 750 °C, both ohmic (R_{ohm}) and polarization resistance (R_p) presented increasing trends. These phenomena could be ascribed to the increased ohmic loss from the electrolyte and electrode components, and reduced electrochemical properties of the electrodes (e.g., fuel oxidation at the anode and oxygen reduction at the cathode). Thus, the maximum power density displayed a corresponding decrease

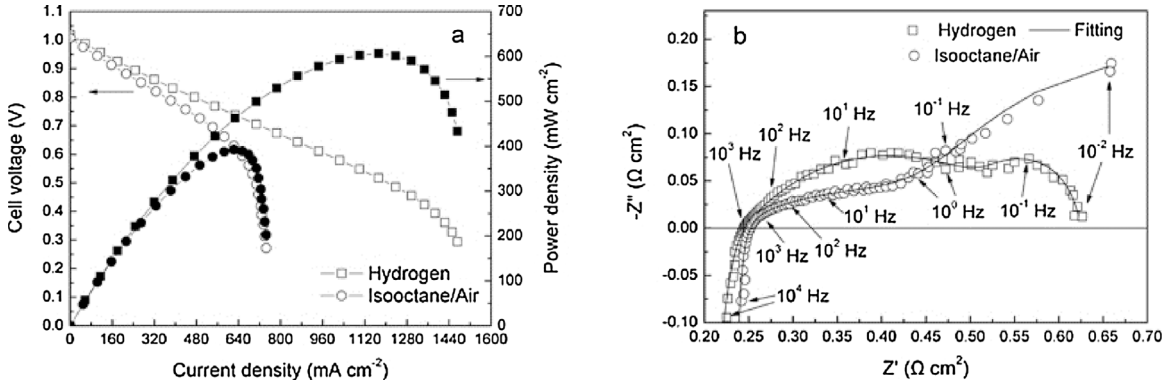

Fig. 6. Electrochemical performance of the single cell without the micro-reforming layer at 750 °C: (a) Cell voltage and power density curves and (b) the Nyquist plots under the OCV condition.

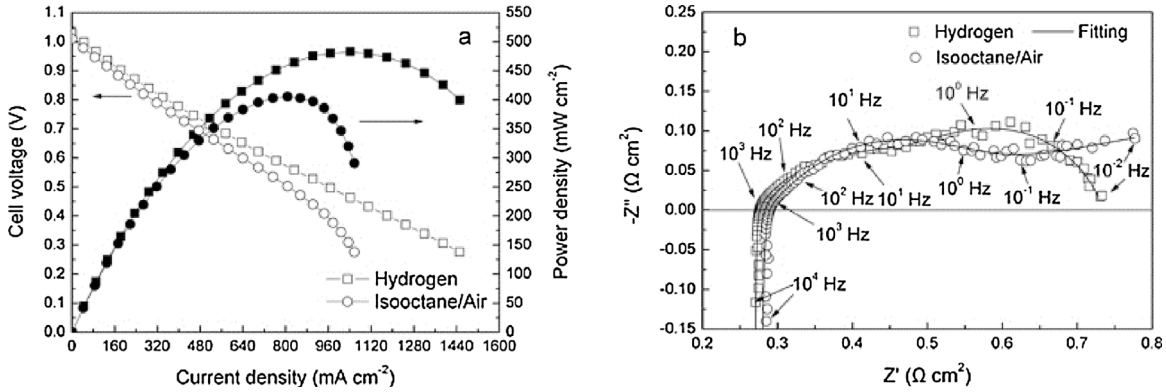

Fig. 7. (a) Cell voltage and power density of the single cell with the micro-reforming layer at 750 °C in hydrogen and isooctane/air, and (b) Nyquist plots of the single cell with the micro-reforming layer under OCV condition.

Table 2
Electrochemical parameters of the single cell with the micro-reforming layer at 750 °C.

Fuel	R_{ohm} (Ω cm^2)	R_H (Ω cm^2)	R_L (Ω cm^2)	R_p (Ω cm^2)	MPD (mW cm^{-2})
Hydrogen	0.26	0.24	0.23	0.47	479
Isooctane/air	0.27	0.21	1.15	1.36	405

from 670 to 606 mW cm^{-2}.

Fig. 6 shows electrochemical performance of the single cell (without the micro-reforming layer) in isooctane/air. The OCV of the single cell was 1.02 V in hydrogen fuel, and it dropped to 1.00 V when switching the fuel from hydrogen to isooctane/air. The variation of the OCV can be ascribed to the changes of gas composition in the anode [22]. The maximum power density dropped by 35% (from 606 to 392 mW cm^{-2}) at 750 °C when changing the fuel from hydrogen to isooctane/air. Since the electrochemical performance was measured immediately after isooctane/air was introduced into the cell, we believe that the coking is not the main cause of the initial drop in the maximum power density. As seen from Fig. 6(b) and Table 1, the single cell exhibited significantly increased polarization resistance (R_p) when switching the fuel from hydrogen to isooctane/air. This higher polarization resistance could be ascribed to the large electrode polarization from gas adsorption and dissociation, and gas diffusion processes (R_L). As shown in Fig. 4(a), with no reforming layer applied in the Ni-YSZ anode, the concentrations of H_2 and CO in the anode were fairly low. The low syngas yield resulted in the evident mass transport limitation at high current densities (> 640 mA cm^{-2}), which led to the drop in the maximum power density.

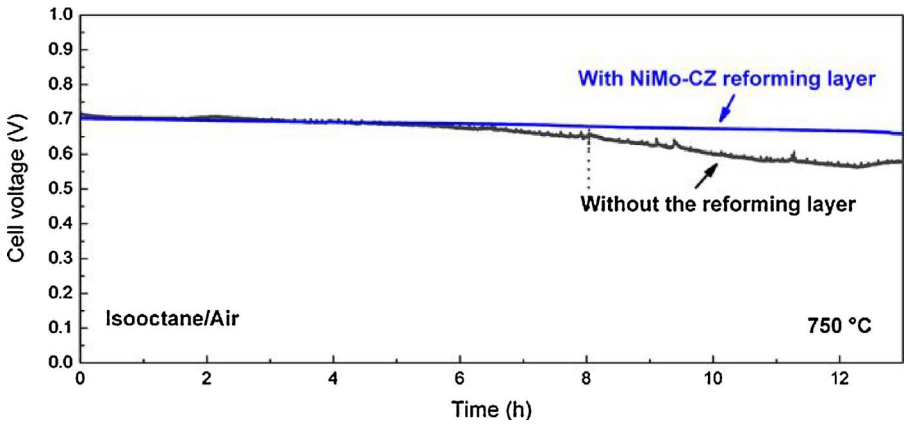

Fig. 8. Performance stability of the single cell with and without the micro-reforming layer in isooctane/air at 750 °C.

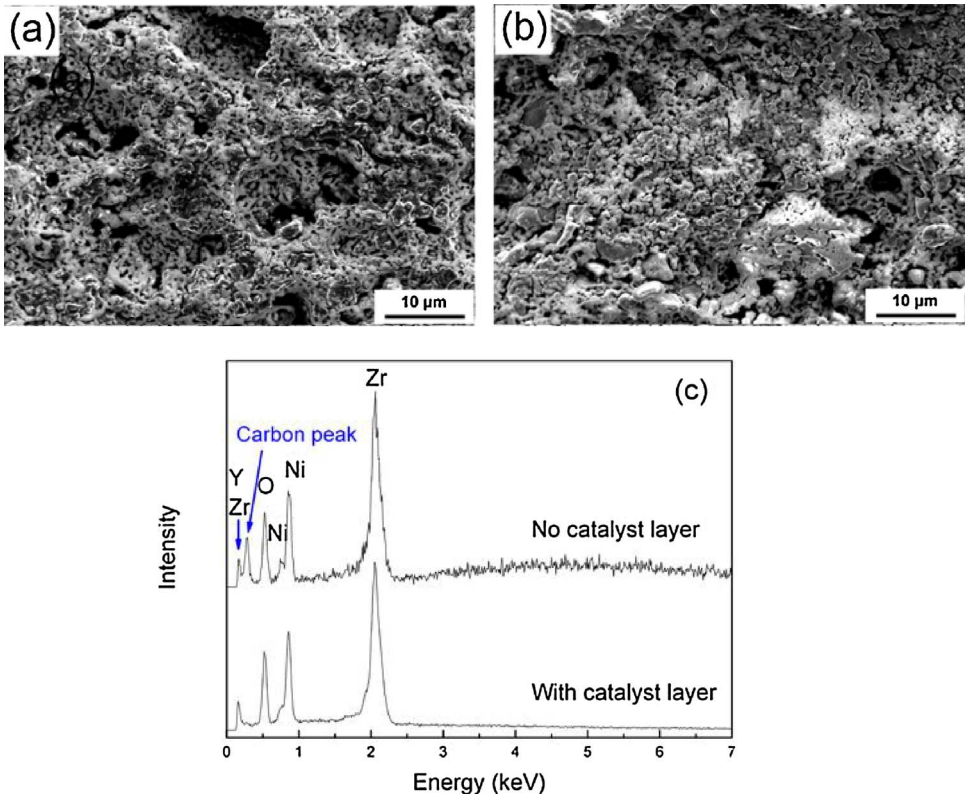

Fig. 9. SEM images of the Ni-YSZ cermet (the surface of the anode) after the performance stability measurement: (a) with the catalyst layer and (b) without the catalyst layer. (c) EDX analyses from (a) and (b).

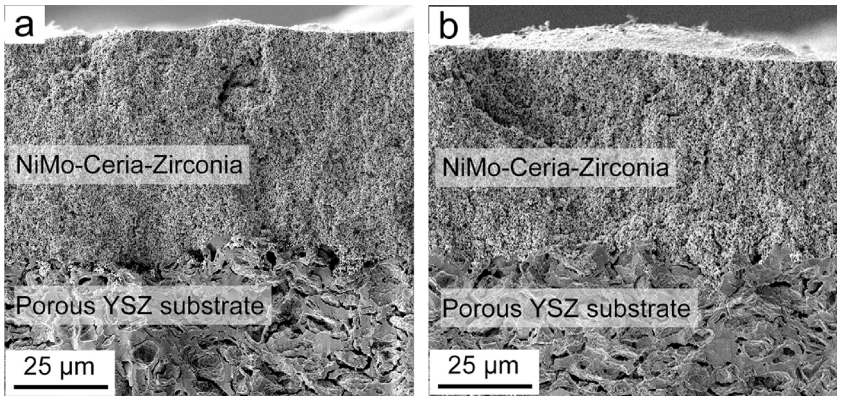

Fig. 10. SEM images of the YSZ substrate coated with NiMo-CZ catalyst: (a) before the stability test and (b) after the stability test.

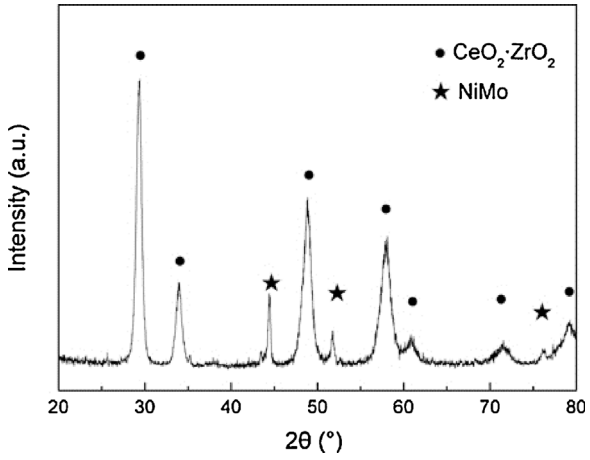

Fig. 11. XRD pattern of NiMo-CZ micro-reforming layer after the stability test.

Fig. 7 shows electrochemical performance of the single cell with the micro-reforming layer at 750 °C in hydrogen and isooctane/air, respectively. Similar to the single cell without the micro-reforming layer, the OCV of the single cell with the micro-reforming layer was 1.03 V in hydrogen fuel, and it dropped to 1.01 V when switching the fuel from hydrogen to isooctane/air. The maximum power density of the single cell with the micro-reforming layer decreased from 479 to 405 mW cm^{-2} at 750 °C (a 15% drop) with the change of the fuel. Comparing to the single cell without the micro-reforming layer, the loss of maximum power density decreased from 35% to 15% by applying the catalytic micro-reforming layer on top of the anode. This reduced power density drop illustrates that the presence of the micro-reforming layer enhances electrochemical performance of the single cell under the isooctane/air operating mode. From our previous work, NiMo-CZ demonstrated a high reforming activity and stability towards the partial oxidation of isooctane, and the reforming activity was also validated in the catalytic reforming layer/anode layer single cell under the OCV condition [25]. By directing the isooctane/air mixture to flow through the NiMo-CZ-based catalytic layer before it reached the Ni-YSZ anode,

we can effectively convert this complex hydrocarbon into simple syngas for electrochemical oxidation. Consequently, Fig. 6 (a) and Fig. 7 (a) clearly demonstrate that the mass transfer polarization for the single cell with the micro-reforming layer is significantly reduced at the high current densities compared to that of the single cell without the micro-reforming layer.

Fig. 7 (b) shows Nyquist plots of the single cell with the micro-reforming layer under hydrogen and isooctane/air, respectively, at 750 °C. The impedance spectra fitting results are listed in Table 2. The single cell with the micro-reforming layer exhibited similar ohmic resistances (0.26–0.27 Ω cm^2) in hydrogen and isooctane/air fuels, while the polarization resistance (R_p) increased from 0.47 to 1.36 Ω cm^2 as the fuel is switched from hydrogen to isooctane/air. However, it is very important to point out that the polarization resistance of the single cell with the micro-reforming layer in isooctane/air (R_p = 1.36 Ω cm^2 at 750 °C in Fig. 7(b) and Table 2) was still much lower than the cell without the reforming layer (R_p: 1.77 Ω cm^2 at 750 °C in Fig. 6(b) and Table 1). This phenomenon further confirmed the reforming function of the NiMo-CZ catalyst layer for effectively converting heavy hydrocarbon fuels and their fragments to simple molecules. Thus, due to the reforming function of the catalyst layer, the higher concentration of syngas would be delivered to the electrochemical region of the anode, which reduced the polarization resistance of the single cell.

Fig. 8 shows performance stability of the single cell with and without the micro-reforming layer under the isooctane/air operation mode. Stability was tested at the constant current density of 500 mA cm^{-2} at 750 °C. The two single cells exhibited comparable performance in the initial 6 h stability test. After 6 h, an evident performance degradation (16.4 mV h^{-1}) was observed for the cell without the micro-reforming layer. With the application of the catalytic micro-reforming layer, the cell performance displayed greatly decreased deterioration rate of 3.0 mV h^{-1}. Moreover, the low degradation rate was comparable with the nickel-containing anode supported single cell without the reforming layer running on simple methane fuel [26,34]. The results demonstrated the capability of the NiMo-CZ-reforming layer for improving performance stability of SOFC running under the direct isooctane/air feeding condition.

3.4. Post-test analysis

After the performance stability measurement, we analyzed the anodes of the single cells with SEM/EDX. Fig. 9 shows that the single cells with and without the micro-reforming layer exhibited similar microstructures, while different carbon amounts were detected by EDX. The anode with no micro-reforming layer presented a high carbon amount (26 wt.%), which could be attributed to coking under the isooctane/air operation mode [35]. With the application of the micro-reforming layer, only 8 wt.% carbon was identified in the anode of the single cell. The results indicated the effectiveness of the micro-reforming layer for directly processing the heavy hydrocarbons and suppressing the carbon deposition in the main Ni-YSZ electrode surface.

Fig. 10 compares SEM images of porous YSZ coated with NiMo-CZ catalyst before and after the performance stability test. The thickness of the YSZ substrate is ~0.4 mm, while the thickness of the NiMo-CZ catalyst layer was determined to be 60 ± 4 μm for the fresh sample. After the stability test, the thickness of the catalyst layer was reduced to be 50 ± 3 μm.

Fig. 11 shows the XRD pattern of the NiMo-CZ-reforming layer after the performance stability test. Only NiMo and CZ phases were detected within the sensitivity of the measurement. Furthermore, there was no diffraction peak at 2θ = 26.6°, which is a good indication for the absence of graphitic carbon. These results illustrated the stability of the NiMo-CZ catalyst and its high coking resistance when it was subjected to the internally reforming condition of isooctane/air. Our findings substantiate the application feasibility of the NiMo-CZ-based micro-reforming layer for running SOFC single cell in isooctane/air.

4. Conclusions

The NiMo-CZ catalyst was successfully applied as the micro-reforming layer for conventional Ni-YSZ anode supported single cell running under the direct isooctane/air feeding mode. Application of the novel catalyst layer was found be an effective way to enhance the electrochemical performance of the single cell under the isooctane/air operating mode. Due to the reforming functions of the NiMo-CZ catalyst layer, the increased amount of synthesis gas can be delivered to the anode of the single cell for electrochemical oxidation, which reduced the polarization resistance from 1.77 to 1.36 Ω cm^2 at 750 °C. As a result, the initial cell performance loss was reduced from 35% to 15% when changing the fuel from hydrogen to isooctane/air. This phenomenon indicated the function of the NiMo-CZ micro-reforming layer on improving the initial performance of the single cell in isooctane/air. In addition, stability of the single cells with and without the micro-reforming layer was compared. During the 12 h test at the constant current density of 500 mA cm^{-2}, the cell with the NiMo-CZ micro-reforming layer presented a much lower voltage degradation rate (3.0 mV h^{-1}) than the cell with no micro-reforming layer (16.4 mV h^{-1}). Furthermore, after the performance stability test, less carbon was detected in the Ni-YSZ anode with the micro-reforming layer. The results support the effectiveness of the NiMo-CZ catalyst layer for suppressing carbon deposition in the Ni-YSZ anode and improving performance stability of the single cell in isooctane/air.

Acknowledgments

This work was supported financially by the National Science Foundation GOALI Program (Grant No. CBET-1034308), the Office of Naval Research (Grant No. N00014-15-1-2416) and Boeing Commercial Airplanes. This work was also supported by Ministry of Science, ICT and Future Planning (MSIP) Republic of Korea.

References

[1] S. McIntosh, R.J. Gorte, Direct hydrocarbon solid oxide fuel cells, Chem. Rev. 104 (2004) 4845–4866.
[2] W.Z. Zhu, S.C. Deevi, A review on the status of anode materials for solid oxide fuel cells, Mater. Sci. Eng. A 362 (2003) 228–239.
[3] M. Cimenti, J. Hill, Direct utilization of liquid fuels in SOFC for portable applications: challenges for the selection of alternative anodes, Energies 2 (2009) 377–410.
[4] T. Hibino, A. Hashimoto, T. Inoue, J.I. Tokuno, S.I. Yoshida, M. Sano, A low-operating-temperature solid oxide fuel cell in hydrocarbon-air mixtures, Science 288 (2000) 2031–2033.
[5] H. Kim, S. Park, J.M. Vohs, R.J. Gorte, Direct oxidation of liquid fuels in a solid oxide fuel cell, J. Electrochem. Soc. 148 (2001) A693–A695.
[6] C. Yang, Z. Yang, C. Jin, G. Xiao, F. Chen, M. Han, Sulfur-tolerant redox-reversible anode material for direct hydrocarbon solid oxide fuel cells, Adv. Mater. 24 (2012) 1439–1443.
[7] H. Kishimoto, Y.-P. Xiong, K. Yamaji, T. Horita, N. Sakai, M.E. Brito, H. Yokokawa, Direct feeding of liquid fuel in SOFC, ECS Trans. 7 (2007) 1669–1674.
[8] K. Kendall, M. Slinn, J. Preece, Formulating liquid ethers for microtubular SOFCs, J. Power Sources 157 (2006) 750–753.
[9] Z.F. Zhou, R. Kumar, S.T. Thakur, L.R. Rudnick, H. Schobert, S.N. Lvov, Direct oxidation of waste vegetable oil in solid-oxide fuel cells, J. Power Sources 171 (2007) 856–860.
[10] J.H. Koh, Y.S. Yoo, J.W. Park, H.C. Lim, Carbon deposition and cell performance of Ni-YSZ anode support SOFC with methane fuel, Solid State Ionics 149 (2002) 157–166.
[11] G. Kaur, S.C.E.R.R. Basu, Physical characterization and electrochemical performance of copper–iron–ceria–YSZ anode-based SOFCs in H2 and methane fuels, Int. J. Energ. Res. 39 (2015) 1345–1354.
[12] S. Kim, C. Kim, J.H. Lee, J. Shin, T.-H. Lim, G. Kim, Tailoring Ni-based catalyst by alloying with transition metals (M = Ni, Co Cu, and Fe) for direct hydrocarbon utilization of energy conversion devices, Electrochim. Acta 225 (2017) 399–406.
[13] M. Miyake, S. Matsumoto, M. Iwami, S. Nishimoto, Y. Kameshima, Electrochemical performances of $Ni_{1-x}Cu_x$/SDC cermet anodes for intermediate-temperature SOFCs using syngas fuel, Int. J. Hydrogen Energy 41 (2016) 13625–13631.
[14] S. Park, R.J. Gorte, J.M. Vohs, Applications of heterogeneous catalysis in the direct oxidation of hydrocarbons in a solid-oxide fuel cell, Appl. Catal. A: Gen. 200 (2000) 55–61.
[15] S. Park, J.M. Vohs, R.J. Gorte, Direct oxidation of hydrocarbons in a solid-oxide fuel cell, Nature 404 (2000) 265–267.
[16] R.J. Gorte, H. Kim, J.M. Vohs, Novel SOFC anodes for the direct electrochemical

oxidation of hydrocarbon, J. Power Sources 106 (2002) 10–15.
[17] R.J. Gorte, J.M. Vohs, Novel SOFC anodes for the direct electrochemical oxidation of hydrocarbons, J. Catal. 216 (2003) 477–486.
[18] S. Jung, C. Lu, H. He, K. Ahn, R.J. Gorte, J.M. Vohs, Influence of composition and Cu impregnation method on the performance of Cu/CeO_2/YSZ SOFC anodes, J. Power Sources 154 (2006) 42–50.
[19] A. Sin, E. Kopnin, Y. Dubitsky, A. Zaopo, A.S. Aricò, D. La Rosa, L.R. Gullo, V. Antonucci, Performance and life-time behaviour of NiCu-CGO anodes for the direct electro-oxidation of methane in IT-SOFCs, J. Power Sources 164 (2007) 300–305.
[20] Z. Xie, C. Xia, M. Zhang, W. Zhu, H. Wang, $Ni_{1-x}Cu_x$ alloy-based anodes for low-temperature solid oxide fuel cells with biomass-produced gas as fuel, J. Power Sources 161 (2006) 1056–1061.
[21] Z. Zhan, S.A. Barnett, An octane-fueled solid oxide fuel cell, Science 308 (2005) 844–847.
[22] Z. Zhan, S.A. Barnett, Solid oxide fuel cells operated by internal partial oxidation reforming of iso-octane, J. Power Sources 155 (2006) 353–357.
[23] G. Bae, J. Bae, P. Kim-Lohsoontorn, J. Jeong, Performance of SOFC coupled with n-C_4H_{10} autothermal reformer: carbon deposition and development of anode structure, Int. J. Hydrogen Energy 35 (2010) 12346–12358.
[24] T. Hibino, A. Hashimoto, M. Yano, M. Suzuki, M. Sano, Ru-catalyzed anode materials for direct hydrocarbon SOFCs, Electrochim. Acta 48 (2003) 2531–2537.
[25] Q. Bkour, K. Zhao, L. Scudiero, D.J. Han, C.W. Yoon, O.G. Marin-Flores, M.G. Norton, S. Ha, Synthesis and performance of ceria-zirconia supported Ni-Mo nanoparticles for partial oxidation of isooctane, Appl. Catal. B: Environ. 212 (2017) 97–105.
[26] B. Han, K. Zhao, X. Hou, D.J. Kim, B.H. Kim, S. Ha, M.G. Norton, Q. Xu, B.G. Ahn, Ni-$(Ce_{0.8-x}Ti_x)Sm_{0.2}O_{2-\delta}$ anode for low temperature solid oxide fuel cells running on dry methane fuel, J. Power Sources 338 (2017) 1–8.
[27] J.C. Slater, Atomic radii in crystals, J. Chem. Phys. 41 (1964) 3199–3204.
[28] B. Huang, X.F. Ye, S.R. Wang, H.W. Nie, R.Z. Liu, T.L. Wen, Performance of Ni/ScSZ cermet anode modified by coating with $Gd_{0.2}Ce_{0.8}O_2$ for a SOFC, Mater. Res. Bull. 42 (2007) 1705–1714.
[29] C. Lalanne, F. Mauvy, E. Siebert, M.L. Fontaine, J.M. Bassat, F. Ansart, P. Stevens, J.C. Grenier, Intermediate temperature SOFC single cell test using $Nd_{1.95}NiO_{4+\delta}$ as cathode, J. Eur. Ceram. Soc. 27 (2007) 4195–4198.
[30] Q.A. Huang, R. Hui, B. Wang, J. Zhang, A review of AC impedance modeling and validation in SOFC diagnosis, Electrochim. Acta 52 (2007) 8144–8164.
[31] K. Zhao, K.S. Lee, M. Chen, B.H. Kim, Q. Xu, B.G. Ahn, Electrochemical performance of a copper-impregnated Ni–$Ce_{0.8}Sm_{0.2}O_{1.9}$ anode running on methane, Int. J. Hydrogen Energy 38 (2013) 3750–3756.
[32] S.P. Jiang, S.P.S. Badwal, An electrode kinetics study of H_2 oxidation on Ni/Y_2O_3-ZrO_2 cermet electrode of the solid oxide fuel cell, Solid State Ionics 123 (1999) 209–224.
[33] E.C. Shin, P.A. Ahn, H.H. Seo, J.M. Jo, S.D. Kim, S.K. Woo, J.H. Yu, J. Mizusaki, J.S. Lee, Polarization mechanism of high temperature electrolysis in a Ni-YSZ/YSZ/LSM solid oxide cell by parametric impedance analysis, Solid State Ionics 232 (2013) 80–96.
[34] K. Zhao, Y. Du, Calcium-doped ceria materials for anode of solid oxide fuel cells running on methane fuel, J. Power Sources 347 (2017) 79–85.
[35] M. Liu, Y. Choi, L. Yang, K. Blinn, W. Qin, P. Liu, M. Liu, Direct octane fuel cells: a promising power for transportation, Nano Energy 1 (2012) 448–455.